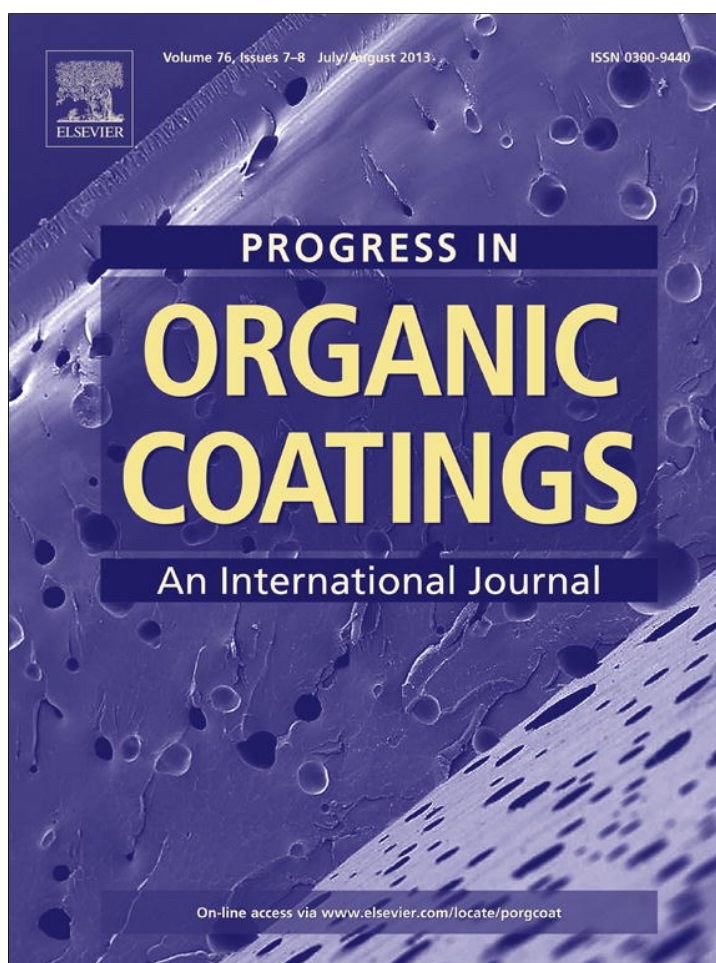


Provided for non-commercial research and education use.  
Not for reproduction, distribution or commercial use.



This article appeared in a journal published by Elsevier. The attached copy is furnished to the author for internal non-commercial research and education use, including for instruction at the authors institution and sharing with colleagues.

Other uses, including reproduction and distribution, or selling or licensing copies, or posting to personal, institutional or third party websites are prohibited.

In most cases authors are permitted to post their version of the article (e.g. in Word or Tex form) to their personal website or institutional repository. Authors requiring further information regarding Elsevier's archiving and manuscript policies are encouraged to visit:

<http://www.elsevier.com/authorsrights>



Contents lists available at SciVerse ScienceDirect

## Progress in Organic Coatings

journal homepage: [www.elsevier.com/locate/porgcoat](http://www.elsevier.com/locate/porgcoat)

## Linseed-oil-based waterborne UV/air dual-cured wood coatings

Chia-Wei Chang, Kun-Tsung Lu\*

Department of Forestry, National Chung Hsing University, 250 Kuo-Kuang Rd., Taichung 402, Taiwan

## ARTICLE INFO

## Article history:

Received 1 November 2012

Received in revised form 26 February 2013

Accepted 27 February 2013

Available online 25 March 2013

## Keywords:

Dual-cured

Linseed oil

Wood coatings

Water-borne polyurethane dispersion

## ABSTRACT

The synthesis of linseed oil (LO)-based waterborne polyurethane dispersion (PUD) wood coatings using different curing processes, as well as their coating and film properties, were examined. The waterborne prepolymer was synthesized first from modified linseed oil (MLO), dimethylol propionic acid (DMPA), isophorone diisocyanate (IPDI), hexamethylene diisocyanate (HDI) and hydroxyethyl methacrylate (HEMA) using an acetone process to prepare a solvent-borne prepolymer with C=C bonds derived from methacrylic acid and fatty acids. The prepolymer was subsequently neutralized with triethylamine (TEA) and dispersed in water. After removing acetone, PUD was obtained. The results showed that the PUD could be readily synthesized and that it possessed reactive double bonds derived from HEMA and LO. Wood coatings were formulated by mixing PUD with photoinitiator for UV curing alone or by mixing PUD with metal dryers for air drying alone or by combining PUD with the two formulations as UV/air and air/UV dual-cured systems. The waterborne wood coatings were cured through different curing processes, as previously mentioned, and the properties of the cured films were characterized. The results showed that the durability and the lightfastness of films prepared using the UV/air dual-curing process (i.e., first UV-cured, followed by air drying) were better than those of the coatings cured using UV alone. Furthermore, the poor adhesion of the films cured using UV alone was significantly improved through the use of the UV/air dual-curing system. In conclusion, the linseed-oil-based waterborne UV/air dual-cured coatings possess the potential to provide high-efficiency, high-performance and environmentally friendly coatings for furniture finishing and it is a candidate for the application of coatings in the wood industry.

© 2013 Elsevier B.V. All rights reserved.

## 1. Introduction

In Taiwan, most of the common solvent-borne wood coatings used in the furniture industry, including nitrocellulose (NC) lacquer, polyurethane (PU) and acrylate lacquer, contain large volumes of volatile organic compounds (VOCs) and hazardous air pollutants (HAPs), which are harmful to the environment and to human health. Furthermore, the unnecessary cost of solvents decreases the profits of the furniture industry. Therefore, environmentally friendly coatings or compliant coatings, such as high-solid-content coatings, waterborne coatings, radiation-curable coatings and powder coatings, have been considered as substitutes for the traditional solvent-borne coatings [1,2].

Among the compliant coatings, waterborne coatings and UV-radiation-curable coatings are ripe for future innovations and for the further development for the furniture industry in Taiwan. In addition, the high cost of fuel and its depletion have significantly increased material costs and have generated serious environmental concerns. To reduce the reliance on petrochemicals, both the

use of renewable resources, such as natural linseed oil, to replace petroleum derivatives for the manufacture of resins and the use of water instead of solvents are imperative.

Compared with the traditional UV coatings, waterborne UV coatings exhibit several benefits. For example, waterborne UV coatings do not rely on the presence of a low-molecular-weight monomer to maintain a low viscosity; they can be prepared using higher-molecular-weight prepolymers and with a smaller amount of total solids; they exhibit lower toxicity/odor and coating shrinkage during the curing process; they are easy to clean up; and they can be applied using conventional application equipment. However, the application of waterborne UV coatings, like the application of traditional UV coatings, is limited to small, simple shapes, such as table tops, doors and wood panels in flat objects, because a coated substrate with a complicated configuration results in shadow zones in the absence of UV radiation, which leads to incomplete curing of the coatings. With such an applicative restriction, waterborne UV coatings could not satisfy the requirements of the furniture market in Taiwan in terms of the variety and quality of the products. In recent years, the modification of UV curing equipment for furniture with complicated configurations has been investigated; however, such equipment is difficult to operate for the production of complicated objects. In addition, traditional UV coatings exhibit

\* Corresponding author. Tel.: +886 4 22840345; fax: +886 4 22873628.  
E-mail address: [lukt@nchu.edu.tw](mailto:lukt@nchu.edu.tw) (K.-T. Lu).

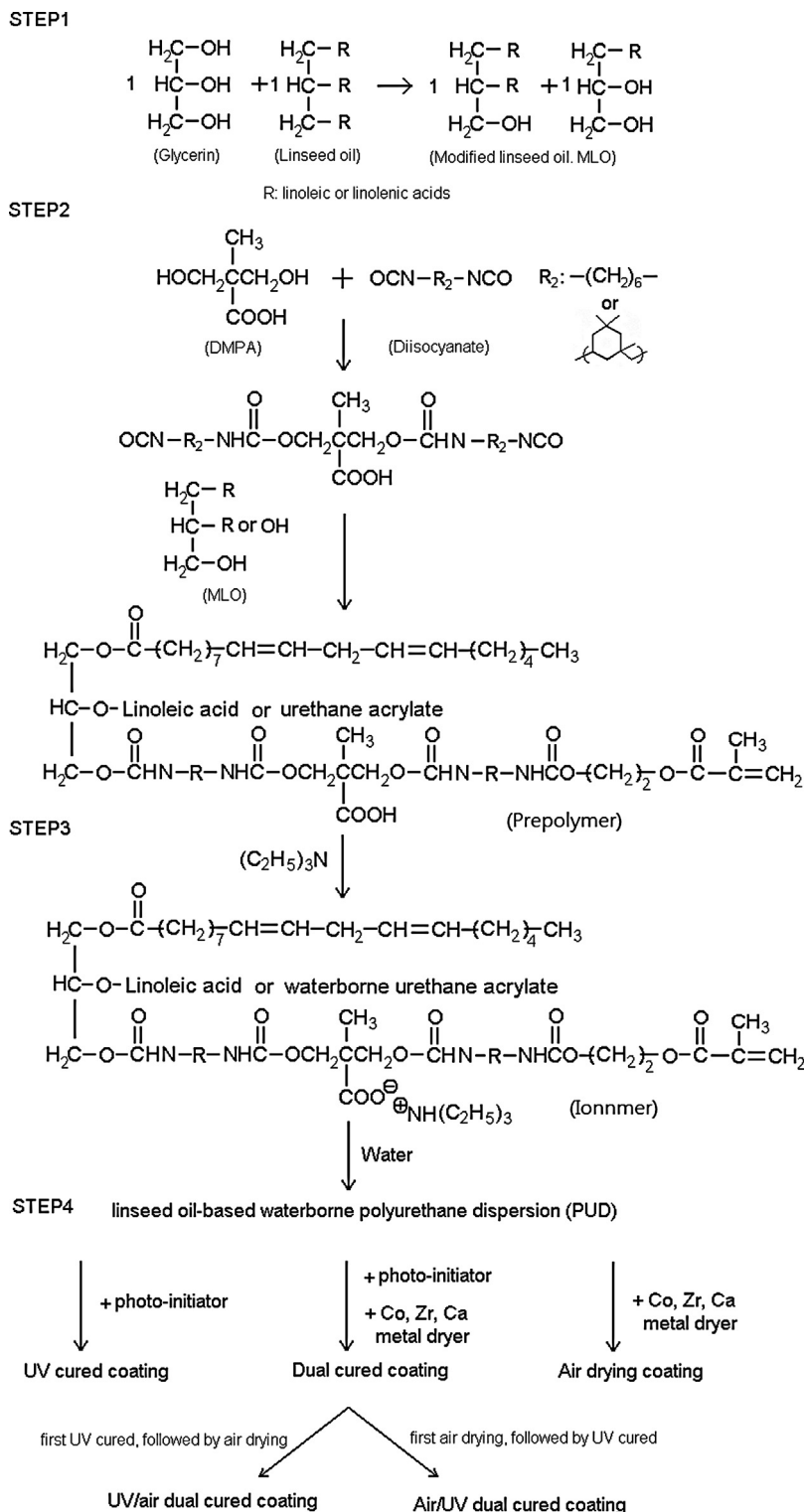


Fig. 1. Synthesis of the prepolymer and the formation of PUD coatings using different curing processes.

defects, such as cured films with non-uniform crosslinking, high internal stress, and oxygen inhibition during the curing process [3–5]. Therefore, the dual-cured coating system that consists of UV curing and air drying, which enables curing of areas that UV radiation cannot reach, is the key to the development of high-quality UV wood coatings.

In this study, linseed oil, which contains unsaturated fatty acids such as linoleic and linolenic acids, was combined with an

OH-containing methacrylate that contains acryloyl double bonds ( $\text{CH}_2=\text{CHCO}$ ) to develop a waterborne polyurethane dispersion (PUD) and to formulate a UV/air dual-cured system that could provide rapid UV curing by free-radical polymerization via UV radiation and slow air drying by an oxidation polymerization process under the shadow zone that is not exposed to UV radiation. Furthermore, the UV-cured films could be further enhanced by a post-curing oxidation polymerization in this system. In

addition, the deposition of linseed-oil-based films can be continued for a period of time and allowed to harden through oxidation polymerization of the unsaturated fatty acids [6]. Compared to the solvent-borne UV/polyurethane (PU) dual-cured system [7], which is a combination of UV curing and a room-temperature curing ability from NCO groups that contains a hardener and polyol, the waterborne UV/air dual-cured system provides a longer pot-life for the coating, greater viscosity stability during finishing and fewer film defects in high-moisture environments. The UV/air dual-cured system is expected to improve the adhesion relative to that achieved with traditional UV coatings, to enhance the application of films on complicated three-dimensional wood products (e.g., furniture) and to form a high-performance film that increases the added value of wood furniture.

## 2. Experimental

### 2.1. Materials

Isophorone diisocyanate (IPDI), hexamethylene diisocyanate (HDI), dimethylol propionic acid (DMPA), and triethylamine (TEA) were obtained from Merck Chemicals, Taiwan. Linseed oil (LO), glycerin, calcium oxide, and acetone were purchased from Union Chemicals, Taiwan. Hydroxyethyl methacrylate (HEMA) was used as a mono-functional monomer and was purchased from Sigma Aldrich, USA. Co, Zr and Ca metal dryers were obtained from Cingyi, Taiwan. Irgacure 2959 was used as a photoinitiator and was obtained from Ciba, Germany. Dibutyltin dilaurate (DBTDL) was supplied by An Fong, Taiwan. All of the chemicals used were of laboratory reagent grade. *Cryptomeria japonica* wood panels with dimensions of 10 cm (*R*) × 15 cm (*L*) × 1 cm (*T*) and a moisture content of 13.0% were used as finishing specimens. Other substrates, such as glass panels, white card paper and Teflon panels, were used to characterize different film properties.

### 2.2. Synthesis of modified linseed oil

To obtain OH groups as reactive sites, modified linseed oil (MLO) was synthesized using a transesterification process with glycerin (GL) and linseed oil (LO) at a molar ratio of 1.0 (GL/LO). A simplified schematic that depicts this reaction is provided in step 1 of Fig. 1. The reaction was performed in a 500 ml four-neck glass reactor equipped with a motorized stirrer, a nitrogen gas inlet tube, a thermometer and one neck for the addition of chemicals. The LO was initially heated to 190 °C within 1 hr under a nitrogen atmosphere. Calcium oxide was added as a catalyst at a weight ratio of 0.2% relative to the LO, and GL was then added dropwise. The mixture was finally heated to 230 °C and stirred for 3 h. To increase the yield of glycerides, the mixture was cooled to room temperature in an ice water bath, and the glycerides were obtained. The hydroxyl number of MLO was measured using the acetic anhydride/pyridine method according to ASTM D1957.

### 2.3. Synthesis of the prepolymer and the waterborne polyurethane dispersion (PUD)

A mixture of 50% DMPA and 50% diisocyanate (IPDI/HDI=1/3) in acetone at a NCO/OH molar ratio of 2.0 was added to a glass reactor, and the reaction was performed at 50 °C for 3 h under a nitrogen atmosphere. Then the calculated 50% HEMA in acetone, equal to the half mole of the residual NCO groups, was added and the reaction was performed at 65 °C for 1 h. When the amount of residual NCO groups reached the quarter amount of initial NCO groups, MLO (with a NCO/OH molar ratio of 1.2 and 50% in acetone) was added dropwise to the mixture at 65 °C over a period of 1 hr. Finally, the mixture was maintained at 65 °C for 3 h and then

cooled to room temperature to obtain the prepolymer. The stirring speed was maintained at 200 rpm throughout the reaction. The schematic depicting this reaction is provided in step 2 of Fig. 1. The solid content, NCO content, appearance, and molecular weight of the prepolymer were characterized, and its FTIR and Raman spectra were collected. Finally, the prepolymer was neutralized with triethylamine (TEA) at a stirring speed of 400 rpm by a dispersion blade, and distilled water was added until the solvent phase was transferred to the aqueous phase (as shown in the step 3 of Fig. 1). After the acetone was removed, PUD was obtained, and its properties, including the solid content, appearance, viscosity, pH value and particle size, were determined.

### 2.4. Preparation of dual-cured coatings

As shown in step 4 of Fig. 1, the UV/air and air/UV dual-cured coatings were prepared by mixing PUD, the photoinitiator (Irgacure 2959, 3% of the weight of the prepolymer), and metal dryers (Co, Zr, and Ca dryers, 0.3% of the weight of the prepolymer). The coating cured using UV alone contained only the Irgacure 2959 photoinitiator, and the coating cured using air-drying alone contained only the Co, Zr, and Ca metal dryers.

### 2.5. Curing processes for the coatings

The coatings were applied onto the substrates using a film applicator with a wet-film thickness of 250 μm. All specimens were placed for 10 min at room temperature and were then transferred to a 50 °C oven for 5 min to remove water. Two experiments were performed with different coatings. In the first experiment, the specimens prepared using UV/air dual-curing and UV curing alone were cured using UV equipment (C-SUN, Taiwan, UVC-362W) with a high-pressure mercury lamp (120 W/cm). The radiation distance was 10 cm, and the conveyer speed was 8 m/min; the curing process was repeated 3 times, which corresponded to an irradiation time of 18 s. The films cured using air/UV dual-curing and air drying alone were first dried at room temperature. After 12 days, the air/UV dual-cured coating specimens were post-cured using UV radiation. The UV curing conditions were the same as those used in the UV curing alone process. All of the film properties were measured after 30 days.

### 2.6. Methods

*Solid content* was estimated in accordance with CNS 5133. *Viscosity* was measured in a Brookfield viscosimeter DV-E at 25 °C. *Fourier-transform infrared spectroscopy (FTIR) analysis* was performed on a Perkin-Elmer spectrum100 spectrophotometer equipped with a DTGS detector. Spectra were recorded with a resolution of 4 cm<sup>-1</sup> and presented as the ratio of 16 single beam scans in a neat KBr window. Liquid samples were diluted in acetone (5% w/w) and applied to a KBr window, and the data were acquired in auto-gain mode to monitor the spectral in the 4000–650 cm<sup>-1</sup> range. The spectra of the liquid and dried film samples were acquired using transmission and attenuated total reflectance (ATR) spectroscopy, respectively. The *molecular weight* and *polydispersity* of the prepolymer were obtained via gel-permeation chromatography (GPC) on a Hitachi D2520 equipped with a Shodex column (Showa Denko, Japan KF-802) at a tetrahydrofuran flow rate of 1 ml/min; poly-styrene standards of molecular masses 162, 578, 1080, 2450, 5050, 10100, 22000; a UV detector were used.; a UV detector was used. The authentic samples of di-glyceride, mono-glyceride and linseed oil were synthesized in our laboratory by transesterification of linseed oil with glycerin. The reaction mixture was analyzed by GPC to identify the corresponding peaks for di-glyceride and mono-glyceride, and the peak of pure linseed oil

was also identified. Raman measurements were performed using a semiconductor laser source operated at 488 nm. The scattered photons were detected by an XYZ scanning-stage system (NT-MDT); the microscope was an inverted microscope (Nikon Eclips TE2000-U). The particle size and the polydispersity index (PDI) of PUD were measured using a Malvern Nano-ZS equipped with laser diffraction and detectors (detected range 0.6 nm–6  $\mu$ m). The pH value of PUD was measured at 25 °C with a pH meter using a glass reference electrode, model Suntlet sp-701. Film hardness was investigated using a König hardness tester (Braive) according to DIN 53157. Tensile strength and elongation at break of free films were evaluated on an EZ Tester (Shimadzu Co.) with a crosshead speed of 5 mm/min. All specimens were cut to a specified shape and size in accordance with ASTM D638. Adhesion on wood panels was determined by the cross-cut method according to CNS K6800 and was divided into the grades 10 (best), 8, 6, 4, 2, and 0 (worst). Impact resistance was determined using a Dupont Impact Tester IM-601, with a falling weight of 300 g and an impact hammer diameter of 0.5 inches. Abrasion resistance of the films was measured in terms of the weight loss of 1000 circles using a Taber Model 503 Abraser; a CS-10 wheel and a load of 500 g were used. Bending resistance of the films was estimated in accordance with CNS 10757-K6801. Gel content was measured using a Soxhlet extractor that contained 250 ml of acetone. The solution was siphoned 24 times in 6 h. The soaked film was dried in an oven at 50 °C for 6 h, and the gel content was calculated. Dynamic mechanical analysis (DMA) was conducted at a frequency of 1 Hz with a DMA8000 (Perkin Elmer, USA). The glass-transition temperature ( $T_g$ ) was determined by the  $\text{Tan}\delta$  curve which was obtained by a tensile mode, at a heating rate of 2 °C/min from –60 to 100 °C under the air atmosphere. Gloss of films was detected using a Dr. Lange Reflectometer 60° gloss meter. Durability of films coated on wood panels was evaluated using hot-and-cold cycles test, in which the specimens were first placed into a –20 °C refrigerator for 2 hr, and then transferred to a 50 °C oven for another 2 h. The cycle number was recorded if the film was cracked. After ten cycles had been performed on the coated specimens, the gloss was measured, and gloss retention was calculated. The lightfastness of films was evaluated with a Paint Coating Fade Meter (Suga Test Instruments, Japan) equipped with a mercury light source (H400-F). After 100 h of exposure, the color changes of the specimens were measured using a spectrophotometer (CM-3600d, Minolta, Osaka, Japan) fitted with a D65 light source with a measuring angle of 10° and a test-window diameter of 8 mm. The tri-stimulus values X, Y, and Z of all specimens were obtained directly from the colorimeter. The CIE  $L^*$ ,  $a^*$ , and  $b^*$  color parameters were then computed, followed by a calculation of the brightness difference ( $\Delta L^*$ ), the color difference ( $\Delta E$ ) and the yellowness difference ( $\Delta YI$ ) directly from the Minolta MCS software system. Thermogravimetric analysis (TGA) was performed using a Perkin-Elmer Pyris 1 system. The films were heated from 50 to 700 °C at a rate of 10 °C/min under a nitrogen atmosphere.

### 3. Results and discussion

#### 3.1. Fundamental properties of the prepolymer

The linseed-oil-based prepolymer was synthesized using acetone as a solvent. The solid content of the prepolymer was 58.6%, and its residual NCO content was 1.0%; it exhibited a transparent yellow color. The GPC spectrum of the prepolymer is presented in Fig. 2. The weight-average molecular weight of 428 g/mole represents the unreacted mono-glyceride, and the molecular weights of 784 and 1070 g/mole represent the prepolymer derived from isocyanates that reacted with DMPA and mono-glyceride or di-glyceride, respectively. In addition, the

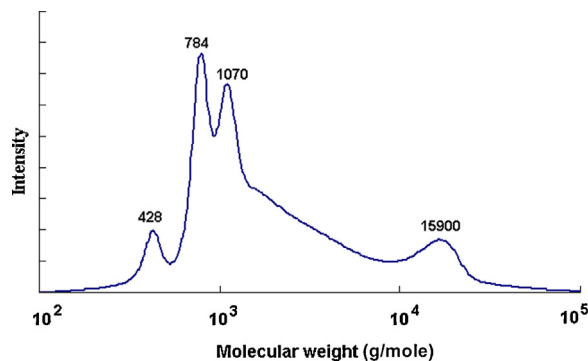


Fig. 2. GPC spectrum of the linseed-oil-based prepolymer.

molecular weight of 15,900 g/mole is attributed to the thermal polymerization (Diels–Alder reaction) product of the unsaturated fatty acids of linseed oil that further reacted with isocyanates to form a urethane-structured product. According to the GPC analysis, the weight-average molecular weight, the number-average molecular weight, and the polydispersity index of the prepolymer were 2943, 1074 g/mole and 2.74, respectively.

The FTIR spectra of the modified linseed oil (MLO) and prepolymer are presented in Fig. 3. Compared to the peak in the spectrum of MLO, the peak at 3446  $\text{cm}^{-1}$  in the spectrum of the prepolymer, which is assigned to the OH group, was significantly weaker, and the spectrum contained peaks at 3340 and 1525  $\text{cm}^{-1}$  assigned to the N–H stretching and bending vibrations, respectively. In addition, the peak that represents the carbonyl (C=O) group was shifted from 1740  $\text{cm}^{-1}$  in the spectrum of MLO to 1718  $\text{cm}^{-1}$  in the spectrum of the prepolymer with an increased absorbance, which indicated the presence of the carboxyl group of DMPA. Furthermore, the absorbance of –NCO groups at 2273  $\text{cm}^{-1}$  was not observed, and peaks at 1239  $\text{cm}^{-1}$  (C–O stretching vibration), 1525  $\text{cm}^{-1}$  (N–H bending vibration), and 1041  $\text{cm}^{-1}$  (C–O stretching vibration), which are attributed to urethane bonds (–NHCO–) of the prepolymer, were detected. The results indicated that the MLO had completely reacted with IPDI, HDI and DMPA to form the prepolymer with urethane linkages and carboxyl groups. However, due to the overlapping absorbance of C=C and C=O in the 1655–1638  $\text{cm}^{-1}$  range, the C=C derived from HEMA or the unsaturated fatty acids could not be easily distinguished in the FTIR spectra. Therefore, the Raman spectrum of the prepolymer was obtained to observe the double bond; the results are presented in Fig. 4.

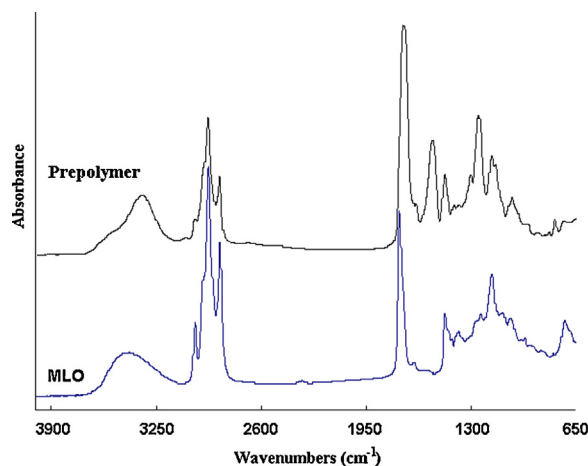


Fig. 3. FTIR spectra of MLO and the prepolymer.

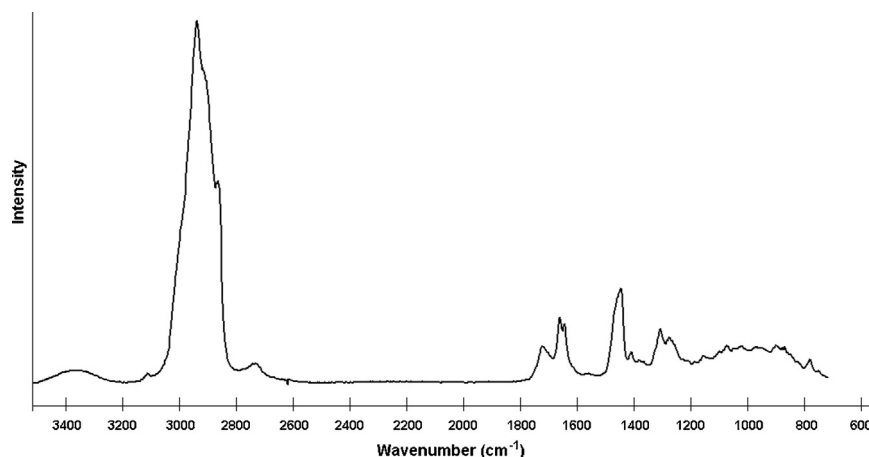


Fig. 4. Raman spectrum of the prepolymer.

In the Raman spectrum of the prepolymer, the peaks at 766, 1276, and 1440  $\text{cm}^{-1}$  were assigned to C–C stretching,  $\text{CH}_2$  out-of-plane bending, and  $\text{CH}_2$  bending vibrations, respectively. In addition, the peak at 1645 was attributed to the C=C of the methacryloyl of HEMA [8] and the peak at 1662  $\text{cm}^{-1}$  was attributed to the unsaturated fatty acids of linseed oil [9]. The broader peak at 1720  $\text{cm}^{-1}$  was produced by C=O, the peak at 1410  $\text{cm}^{-1}$  represented C–O stretching, and the broad peak at 2862–2932  $\text{cm}^{-1}$  was assigned to the C–H stretching vibrations of terminal  $-\text{CH}_2$  and  $-\text{CH}_3$  groups.

### 3.2. Fundamental properties of PUD

PUD was obtained first through neutralization of the prepolymer with TEA at a neutralization degree of 100%, and distilled water was subsequently added under a dispersion blade with a stirring speed of 500 rpm to form an aqueous dispersion, as shown in step 3 of Fig. 1. PUD was obtained after the solvent phase was transferred to the aqueous phase, and the acetone was removed by distillation under reduced pressure. The PUD had a solids content of 36.2%, a transparent yellow appearance, a pH value of 9.14 and a viscosity of 389 cps. The particle size distribution of the PUD, which was analyzed using a laser-scattering particle size distribution analyzer, is shown in Fig. 5. The results showed that the Z-average of PUD was 244.7 nm and that the polydispersity index (PDI) was 0.34. Two particle distribution peaks, at 261 and 5001 nm, were observed, which indicated that the PUD exhibited an inhomogeneous composition. As reported by Nanda [10], PUD with a lower degree of neutralization or a lower carboxylic acid content resulted in a larger and inhomogeneous particle-size composition. However, in our previous report [11], we found that the waterborne castor-oil-based PUD, which was prepared using a similar synthetic process,

exhibited a very small Z-average of 93 nm and a narrow PDI of 0.124. Therefore, in this study, the larger particle composition of linseed-oil-based PUD may be due to thermal polymerization during the transesterification process and due to the formation of a higher molecular weight of heat-bodied linseed oil.

### 3.3. Film properties of PUD coatings with different curing processes

The film properties of PUD coatings prepared using different curing processes, which are shown in step 4 of Fig. 1, are tabulated in Table 1. The air/UV dual-cured coating exhibited the highest hardness of 77 s, followed by the UV/air dual-cured coating, with a hardness of 69 s. The dual-cured systems exhibited a higher hardness than both the coating cured using UV alone. And concerning the hardness the coating cured using air drying alone has also superior results compared to the traditional soybean oil-based UV coating by Chen et al. [12]. The results reflect that the structures of the dual-cured coating films (UV/air and air/UV) possessed both curing mechanisms of the bulk free-radical polymerization and the oxygen-dependent oxidation polymerization during the curing process. Stenberg [13] and Mallégo [14] have stated that air drying results in the formation of a skin layer with a higher crosslinking density.

In the air/UV dual-cured coatings, the first air drying procedure to produce a skin layer with high crosslinking density acted as a diffusion barrier and limited the diffusion of oxygen into the inner layer of the film. This process was followed by rapid UV post-curing, which was the major curing mechanism at the inner layer. The inner layer contained more unsaturated double bonds, and a higher crosslinking density was therefore obtained after UV

Table 1  
Fundamental properties of PUD coating with different curing processes.

Property	Curing process			
	UV	UV/air	Air/UV	Air
Hardness (König, sec)	63 ± 3	69 ± 4	77 ± 2	46 ± 1
Tensile strength ( $\text{kgf}/\text{cm}^2$ )	60 ± 5	81 ± 8	82 ± 1	39 ± 11
Elongation at break (%)	197 ± 14	223 ± 11	223 ± 4	256 ± 6
Impact resistance (cm)	10	15	10	20
Abrasion resistance (mg/1000 circles)	21.8 ± 1.8	18.9 ± 0.6	20.0 ± 1.3	35.0 ± 1.8
Adhesion (grade)	4	10	10	10
Bending resistance	< 2	3	8	6
Gel content (wt. %)	57.4 ± 0.6	61.1 ± 0.3	62.1 ± 0.7	59.8 ± 1.2
Glass transition point, $T_g$ ( $^{\circ}\text{C}$ )	40.6	45.7	36.8	35.9

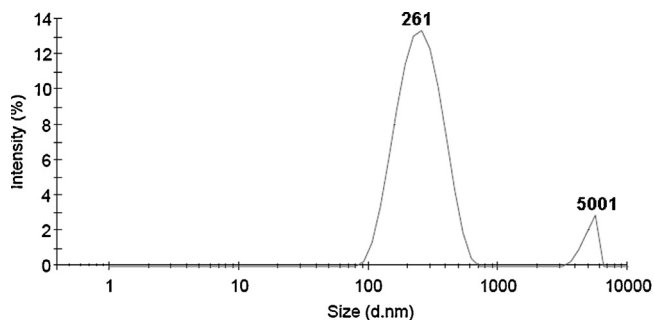


Fig. 5. Particle size distribution of PUD.

post-curing. Because of the interactions of the previously discussed different curing mechanisms, the air/UV dual-cured films had a vertical difference of crosslinking density in the films i.e. the top layer had a higher crosslinking density and the under layer had a lower crosslinking density; however, they also exhibited the highest film hardness.

In the UV/air dual-cured coating, the whole body of the film was cured by the first UV radiation treatment, and a more uniform structure with a lower crosslinking density was obtained. The oxygen subsequently diffused slowly into the inner layer of the film and produced a film with a higher and more uniform crosslinking density during the air-drying post-curing process. However, the UV/air and air/UV dual-cured coatings exhibited similar crosslinking densities for the whole films, the air/UV dual-cured coating exhibited a greater difference in the crosslinking density between the inner part and skin layer of the film. The results revealed that the air/UV dual-cured coating exhibited higher film hardness than did the UV/air dual-cured coating. A similar effect was observed for the dual-cured process in a UV/PU dual-cured coating, as previously reported [7].

The tensile strengths of the two dual-cured coatings (UV/air and air/UV) were similar (approximately 81–82 kgf/cm<sup>2</sup>) and were higher than that of the coating cured using UV alone (60 kgf/cm<sup>2</sup>) and that of the coating cured using air drying alone (39 kgf/cm<sup>2</sup>). We attributed these results to more extensive crosslinking of the C–C bonds in the dual-cured coatings, which was in accordance with the gel content. The coating cured by air drying alone exhibited the greatest elongation at break (256%), followed by the coatings cured using the UV/air and air/UV dual-curing methods (223%) and the coating cured using UV alone (197%). Compared to the coating cured using UV alone, the UV/air and air/UV dual-cured coatings not only exhibited improved tensile strength but also enhanced elongation at break due to the crosslinking of ductile long alkyl chains of the unsaturated fatty acid through the air-drying process. And compared to the UV-curable vinyl ether functionalized urethane UV coating in the report of Kayaman-Apohan et al. [15], the dual-cured coating in this study has a superior strength and elongation at break. These results were also in accordance with the UV/air and air/UV curing coatings, exhibiting the best adhesion grade of 10, whereas that of the UV coating was only grade 4. The UV coating exhibited the worst adhesion was due to the high internal stress and shrinkage in a fast curing process. Compared to the tung-oil based acrylated urethane UV coatings by Lu and Wu [16], the dual-cured coating has an excellent adhesion of film, and the adhesion of the coating cured using UV alone in this study could obviously be improved through the use of a UV/air dual-curing method.

The coating cured using air drying alone exhibited the highest impact resistance of 20 cm, which was attributed to the good ductility of the film. However, the coating cured using air drying alone exhibited the worst abrasion resistance, with a weight loss of 35 mg/1000 circles. Larsen-Badse [17] has stated that the abrasion resistance is interrelated with the material's stress–strain character; the abrasion resistance shows a positive correlation with the area under the stress–strain curve. As shown in Fig. 6, the UV/air and air/UV dual-cured coatings exhibited a greater area under their stress–strain curves, which means they possessed superior abrasion resistance.

The coatings cured using air drying alone and air/UV dual-curing exhibited inferior bending resistance, only passing the no. 6 and no. 8 shafts, respectively. In the bending tests, the films cured using air drying showed an unrecovered and irregular wrinkling mark, which was due to the difference in crosslinking density between the skin and the inner layer of the air-dried films. Therefore, the worst bending resistance of the air/UV dual-cured coating may be derived from the greater crosslinking density of the skin layer as a result of air oxidation polymerization and from the greater internal stress

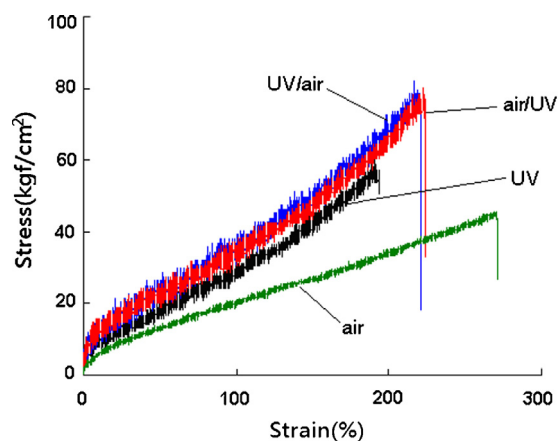


Fig. 6. Stress-strain curves of PUD coatings prepared using different curing processes.

of the inner layer as a result of the UV free-radical polymerization. The coatings cured using air/UV and UV/air dual-curing methods exhibited superior gel contents of 62.1 and 61.1%, whereas the coating cured using UV alone exhibited the lowest gel content of 57.4%. The results indicated that the dual-cured systems, which combined air oxidation polymerization with UV free-radical polymerization, possessed films with a higher crosslinking density. The UV-cured coating contained a slightly lower gel content than did the coating cured using air drying alone; however, the UV cured coating exhibited a higher film hardness and tensile strength, which was attributed to the superior crosslinking and homogeneous structure of the coating cured using UV alone. This conjecture was confirmed by the T<sub>g</sub> (determined by the maximum value of the tan  $\delta$  curves, as shown in Fig. 7) of the coating cured using UV alone (40.6 °C), which was higher than that of the coating cured using air drying alone (35.9 °C). In contrast, the UV/air dual-cured coating exhibited a T<sub>g</sub> of 45.7 °C, which was higher than that of the air/UV dual-cured coating, at 36.8 °C. These results were attributed to the post-cured oxidation polymerization of the UV/air-curing process strengthening the crosslinking structure of the UV-cured film. In contrast, the post-cured UV free-radical polymerization of the air/UV cured process did not effectively increase the crosslinking density of the air-dried film and, furthermore, interfered with the oxidation polymerization of the air-drying process. The results also showed that the air/UV dual-cured coating and the coating cured using air drying alone exhibited similar T<sub>g</sub> values. In addition, shoulder peaks were observed in the tan  $\delta$  curves of both coatings, which indicated that the air/UV dual-curing process resulted in a more heterogeneous structure of films than did the UV curing alone or the UV/air dual-curing process.

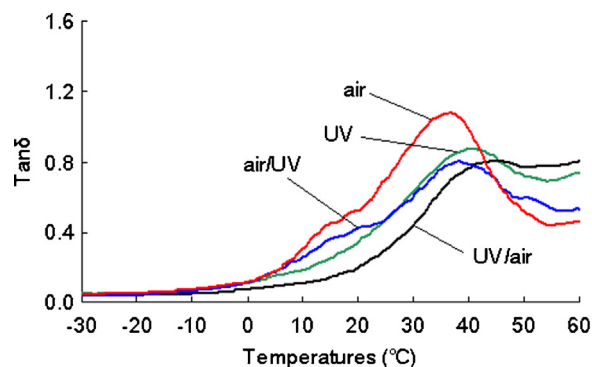


Fig. 7. Tan curves, as determined from DMA analysis, of PUD coatings prepared using different curing processes.

**Table 2**

The gloss, durability and lightfastness of PUD coatings prepared using different curing processes.

Property	UV	UV/air	Air/UV	Air	
60° Gloss (°)	89 ± 0	84 ± 1	84 ± 1	76 ± 2	
Cycle test (rounds)	> 10	> 10	> 10	> 10	
Gloss retention (%)	97	100	90	75	
Lightfastness	$\Delta L^*$	-0.9	-0.3	-0.6	-0.4
	$\Delta E$	2.5	0.5	0.9	1.1
	$\Delta YI$	4.6	0.3	1.4	2.2

The TGA and DTG curves of PUD coatings prepared using different curing processes.

The gloss values of the PUD coatings prepared using different curing processes are listed in Table 2. The coating prepared using air drying alone exhibited the lowest gloss of 76° due to the invisible wrinkling of the film caused by the oxidation polymerization of unsaturated fatty acids of the linseed oil [18]. The other coatings exhibited a superior gloss, especially the coating cured using UV alone, which exhibited the highest gloss of 89°. The results also showed that the air/UV and UV/air dual-cured coatings exhibited better gloss compared to the coating prepared using air drying alone because a smoother film could be obtained through UV irradiation. All specimens also exhibited superior durability, which means that after 10 cycles of hot-and-cold cycling tests, the films remained intact. The UV/air dual-cured coating, in particular, exhibited an excellent gloss retention of 100%.

The lightfastness of PUD coatings prepared using different curing processes after 100 hr of exposure to a mercury lamp is also listed in Table 2. All of the films exhibited a slightly decreased brightness difference ( $\Delta L^*$ ) of approximately -0.9 to -0.3. The color difference ( $\Delta E$ ) of the UV/air dual-cured coating exhibited the lowest  $\Delta E$  value of 0.5, which means it exhibited the best lightfastness among all of the coatings. All of the specimens exhibited small yellowness index difference ( $\Delta YI$ ) values, and, as expected, the coating cured using UV alone exhibited the highest  $\Delta YI$  of 4.6. Lazzari (1999) suggested that the yellowing of linseed-oil-based films was related to the conjugated double bonds produced during the oxidation polymerization process. Mallégol [19] also suggested that hydroperoxides are the key intermediates in the air-drying process and that metal dryers act as catalysts for hydroperoxide decomposition in redox reactions. The free radicals generated from the decomposition of hydroperoxides may react with conjugated double bonds and form a saturated polymer chain. Therefore, the highest  $\Delta YI$  of the coating cured using UV alone was most likely due to the incomplete oxidation polymerization and to the formation

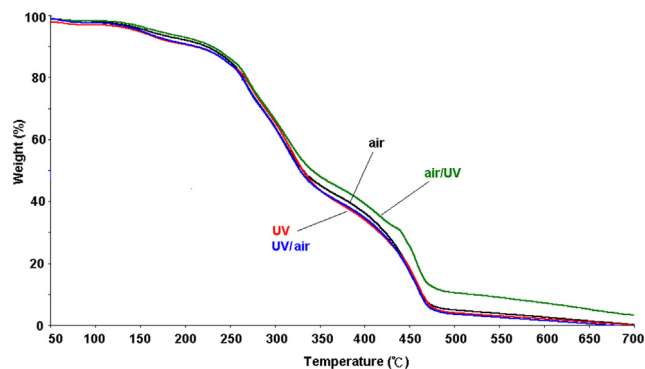


Fig. 8. TG curves of PUD coatings prepared using different curing processes.

of more conjugated double bonds in the film, which resulted in a higher yellowing color. In addition, as reported by O'Neil [20] and Formo [21], the production of diketones, metal salts of their enol form or quinoid structures formed after aging are the primary reasons for the yellowing of linseed-oil-based films.

The TGA and DTG curves of PUD coatings prepared using different curing processes are presented in Fig. 8 and Fig. 9, respectively, and the thermal parameters are summarized in Table 3. The TG curves of specimens were similar, and four stages of thermal degradation were observed. In stage I, an insignificant weight loss at approximately 150 °C was due to the loss of humidity in the films. Stage II showed similar onset temperatures from 248 to 252 °C and similar peak temperatures from 267–271 °C for the specimens. This stage represented the decomposition of the urethane linkage and the formation of -NCO, primary amines, and secondary amines [22]. The weight losses of all specimens in this stage were similar and in the 22.4–26.0% range. Stage III, which began at approximately 299 to 307 °C and exhibited peak temperatures from 312 to 318 °C, was caused by the thermal decomposition of soft fragments, such as the ether or ester bonds of alkyl chains [23]. In this thermal degradation stage, the UV/air dual-cured coating exhibited the lowest weight loss of 29.0%, which indicated that this coating contained the most extensive crosslinking structure; these results were in agreement with the Tg results.

In stage IV, the final stage, an onset temperature from 414 to 443 °C and a peak temperature from 457 to 459 °C were observed, which were attributed to the dehydrogenation and depolycondensation of alkyl groups of PUD coatings [24]. In this stage, the trace of the air/UV dual-cured coating contained an obvious shoulder peak

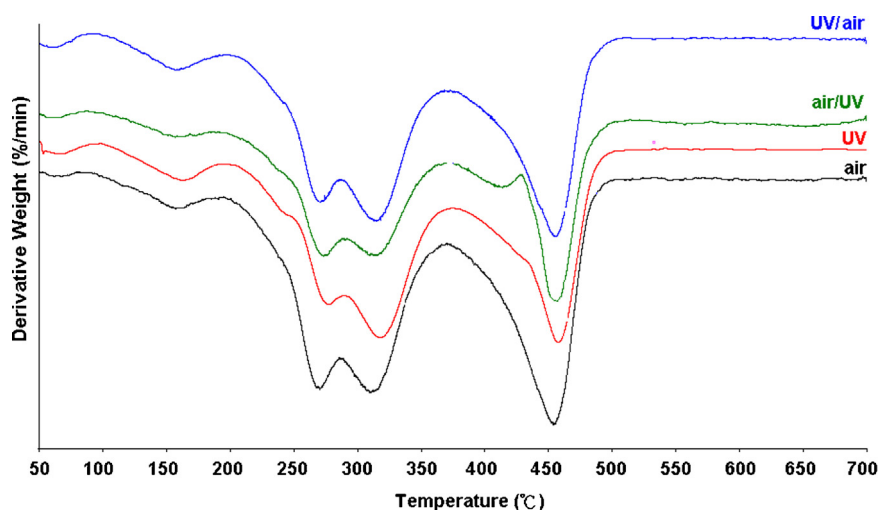


Fig. 9. DTG curves of PUD coatings prepared using different curing processes.

**Table 3**  
Thermal parameters of PUD coatings prepared using different curing processes.

Coatings	Stage II			Stage III			Stage IV			Residue content(% at 700 °C)
	Onset (°C)	Peak temperature (°C)	Weight loss (%)	Onset (°C)	Peak temperature (°C)	Weight loss (%)	Onset (°C)	Peak temperature (°C)	Weight loss (%)	
UV	250	271	24.1	307	318	33.6	428	459	27.7	2.0
UV/air	252	268	24.4	303	314	29.0	414	459	34.3	0.3
Air/UV	248	270	22.4	299	313	36.8	443	457	27.6	4.5
Air	248	267	26.0	301	312	33.6	425	457	30.7	0.0

at 415 °C due to the heterogeneity of the polymer chain arrangement in this coating. The air/UV dual coating exhibited the highest residue content of 4.5% at 700 °C, followed by that of the coating cured using UV alone, at 2.0%, and those of the UV/air dual-cured and air drying alone coatings, at 0.3 and 0.0%, respectively. Based on these results, we concluded that all of the films cured using different curing processes exhibited a similar thermal decomposition behavior; however, the air/UV dual-cured coating exhibited the lowest weight loss in stage II IV and also produced the greatest residue content at 700 °C, thereby exhibiting the best heat resistance among the investigated coatings.

#### 4. Conclusions

In this study, both the synthesis of linseed-oil-based waterborne polyurethane dispersion wood coatings and film performances with different curing processes—including processes where the coating was cured using UV alone, using a UV/air dual-curing method, using an air/UV dual-curing method and using air drying alone—were examined. The UV/air dual-cured coating could be rapidly cured under UV irradiation and could also be dried through oxidation polymerization at areas that lacked exposure to UV radiation. Furthermore, compared to the coating cured using UV alone, the film properties, including the hardness, the tensile strength, the impact resistance, the abrasion resistance, the durability and the gel content, could be enhanced through the use of the UV/air dual-curing process. The film adhesion, in particular, could be improved significantly. Compared to the air/UV dual-cured coating, the UV/air dual-cured coating exhibited superior durability and lightfastness. However, the air/UV dual-cured coating exhibited better hardness, tensile strength, abrasion resistance, durability and heat resistance than the coating cured using air drying alone. We concluded that the UV/air dual-cured coating can effectively overcome the shortcoming of traditional UV coatings and results in a film with excellent performance. This method is suitable for wood finishing, especially for furniture with a complicated configuration.

#### References

- [1] K.D. Weiss, *Prog. Polym. Sci.* 22 (1997) 203–245.
- [2] P.J.A. Geurink, T. Scherer, R. Buter, A. Steenbergen, H. Henderiks, *Prog. Org. Coat.* 55 (2006) 119–127.
- [3] K.T. Lu, *Wood coatings*; book 17 published as a part of a series, *For. Prod. Ind.* (2001) 73.
- [4] D. Benda, J. Šňupárek, V. Čermák, *Eur. Polym. J.* 45 (2001) 1247–1253.
- [5] D.B. Otts, E. Heidenreich, M.W. Urban, *Polym.* 46 (2005) 8162–8168.
- [6] M. Lazzari, O. Chiantore, *Polym. Degrad. Stab.* 65 (1999) 303–313.
- [7] C.W. Chang, K.T. Lu, *J. Appl. Polym. Sci.* 115 (2009) 2197–2202.
- [8] Spectral database for organic compounds (SDBS) web page. <http://sdb.srioddb.aist.go.jp/sdbs/cgi-bin/cre.index.cgi?lang=eng>
- [9] H. Abramczyka, B. Brozek-Pluskaa, J. Surmackia, J. Jablonska-Gajewicz, R. Kordekb, *Prog. Biophys. Molbio.* 108 (2012) 74–81.
- [10] A.K. Nanda, D.A. Wicks, *Polym. J.* 47 (2006) 1805–1811.
- [11] C.W. Chang, K.T. Lu, *Prog. Org. Coat.* 75 (2012) 435–443.
- [12] Z. Chen, J.F. Wu, S. Fernando, K. Jagodzinski, *Prog. Org. Coat.* 71 (2011) 98–109.
- [13] C. Stenberg, M. Svensson, M. Johansson, *Ind. Crop. Prod.* 21 (2005) 263–272.
- [14] J. Mallégol, J. Lemair, J.L. Gardette, *Prog. Org. Coat.* 39 (2000) 107–113.
- [15] N. Kayaman-Apohan, A. Amanoela, N. Arsuc, A. Güngör, *Prog. Org. Coat.* 49 (2004) 23–32.
- [16] K.T. Lu, H.F. Wu, *Quart. J. For. Res. of Taiwan* 30 (2008) 57–66.
- [17] J. Larsen-Badse, K.G. Mathew, *Wear* 4 (1969) 199–205.
- [18] M.D. Soucek, T. Khattab, J. Wu, *Prog. Org. Coat.* 73 (2012) 435–454.
- [19] J. Mallégol, L. Gonon, J. Lemaire, J.-L. Gardette, *Polym. Degrad. Stab.* 72 (2001) 191–197.
- [20] O'Neil, *Los Angeles Paint Technology* 27 (1963) 44.
- [21] M.W. Formo, *Paints, varnishes and related products: discoloration*, in: D. Swern (Ed.), *Bayley's industrial oil and fat products*, vol. I, 4th ed., John Wiley, Chichester, UK, 1979, p. 687.
- [22] I. Javni, Z.S. Petrić, A. Guo, R. Fuller, *J. App. Polym. Sci.* 77 (2000) 1723–1734.
- [23] E. Hablot, D. Zheng, M. Bouquey, L. Avèrous, *Macromol. Mater. Eng.* 293 (2008) 922–929.
- [24] F. Gaboriaud, J.P. Vantelon, *J. Polym. Sci., Polym. Chem. Ed.* 20 (1982) 2063–2071.